ACCOUNTS
of chemical research

Boosting the Efficiency of Quantum Dot Sensitized Solar Cells through Modulation of Interfacial Charge Transfer

PRASHANT V. KAMAT*

Radiation Laboratory, Department of Chemistry and Biochemistry, University of Notre Dame, Notre Dame, Indiana 46556, United States

RECEIVED ON DECEMBER 29, 2011

CONSPECTUS

The demand for clean energy will require the design of nanostructure-based light-harvesting assemblies for the conversion of solar energy into chemical energy (solar fuels) and electrical energy (solar cells). Semiconductor nanocrystals serve as the building blocks for designing next generation solar cells, and metal chalcogenides (e.g., CdS, CdSe, PbS, and PbSe) are particularly useful for harnessing size-dependent optical and electronic properties in these nanostructures.

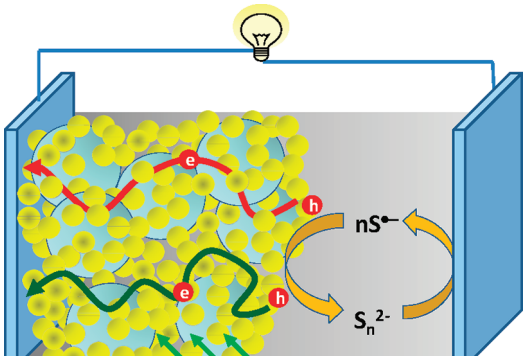

This Account focuses on photoinduced electron transfer processes in quantum dot sensitized solar cells (QDSCs) and discusses strategies to overcome the limitations of various interfacial electron transfer processes. The heterojunction of two semiconductor nanocrystals with matched band energies (e.g., TiO_2 and CdSe) facilitates charge separation. The rate at which these separated charge carriers are driven toward opposing electrodes is a major factor that dictates the overall photocurrent generation efficiency. The hole transfer at the semiconductor remains a major bottleneck in QDSCs. For example, the rate constant for hole transfer is 2−3 orders of magnitude lower than the electron injection from excited CdSe into oxide (e.g., TiO_2) semiconductor. Disparity between the electron and hole scavenging rate leads to further accumulation of holes within the CdSe QD and increases the rate of electron−hole recombination. To overcome the losses due to charge recombination processes at the interface, researchers need to accelerate electron and hole transport.

The power conversion efficiency for liquid junction and solid state quantum dot solar cells, which is in the range of 5−6%, represents a significant advance toward effective utilization of nanomaterials for solar cells. The design of new semiconductor architectures could address many of the issues related to modulation of various charge transfer steps. With the resolution of those problems, the efficiencies of QDSCs could approach those of dye sensitized solar cells (DSSC) and organic photovoltaics.

Assembling semiconductor nanostructures on electrode surfaces in a controlled fashion is an attractive approach for designing next generation solar cells.[1] Quantum dot solar cells in particular have emerged as the potential contender for making transformative changes.[2−7] Three types of configurations, solid state heterojunction, polymer−semiconductor hybrid, and liquid junction quantum dot sensitized solar cells, have emerged as viable candidates (Figure 1). These types of solar cells are based on the charge separation at the interface between excited short bandgap semiconductor and a large bandgap semiconductor (or polymer). The preferred choice of light-absorbing semiconductor nanocrystal has been metal chalcogenides (CdS, CdSe, Sb_2S_3, PbS, and PbSe) because they are easy to prepare using benchtop chemistry and exhibit photostability in solar cells.[8−12]

The ability to control optical and electrical properties of the semiconductor nanocrystals by means of size and shape provides the flexibility to tune the performance of solar cells.[13−16] The sensitization of CdS or CdSe quantum

Published on the Web 04/11/2012 www.pubs.acs.org/accounts
10.1021/ar200315d

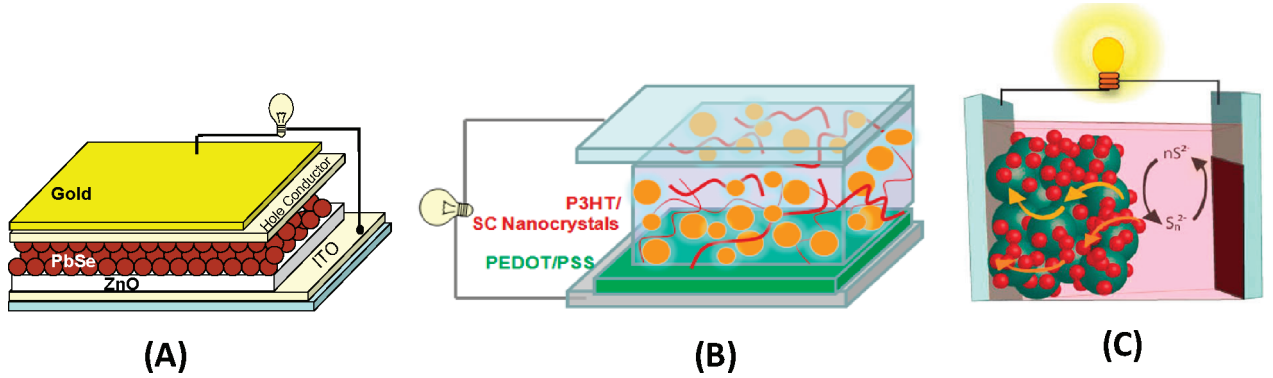

FIGURE 1. Designing solar cells with semiconductor nanocrystals: (A) semiconductor heterojunction; (B) polymer–semiconductor hybrid solar cells; (C) liquid junction solar cells.

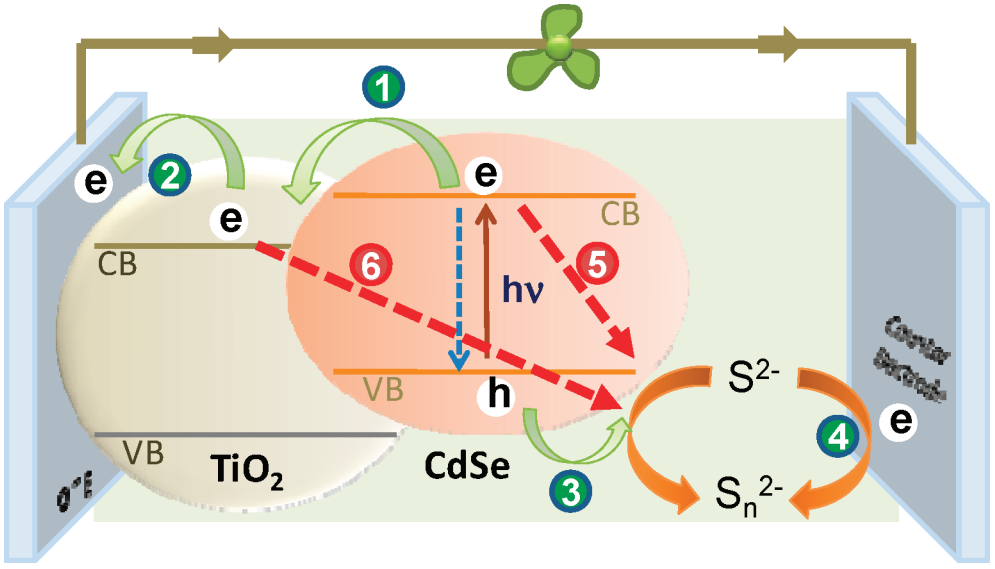

FIGURE 2. Interfacial charge transfer processes that follow excitation of semiconductor nanocrystals in quantum dot sensitized solar cells (QDSCs). See text for description of individual electron transfer steps.

dots on nanocrystalline metal-oxide surfaces (typically TiO_2) is achieved by SILAR (successive ionic layer adsorption and reaction), chemical bath deposition, electrochemical deposition, electrophoresis, and linker-assisted binding.[10,17–25] Because of the porous geometry of the metal oxide film more surface area is available for interaction with excited sensitizer and the penetrating hole scavenger (namely, the redox couple in a quantum dot sensitized solar cell, QDSC). Whereas most recent studies focus on the net photoconversion efficiency of quantum dot solar cells, correlation between various electron transfer steps and the cell performance is still lacking.

In a quantum dot sensitized solar cells, a series of charge transfer processes had to occur cooperatively so that the electrical output can be harnessed efficiently (Figure 2). These include (1) electron injection from excited metal chalcogenide into metal oxide nanoparticle, (2) electron transport to the collecting electrode surface, (3) hole transfer to the redox couple, and (4) regeneration of the redox couple at the counter electrode. A major force that counteracts these favorable processes 1–4 is the charge recombination of electrons at the electrolyte interface (5 and 6 in Figure 2). This Account focuses on the recent progress made in understanding the kinetics and mechanistic aspects of various charge transfer processes at the semiconductor interface and their role in optimization of solar cell performance.

Electron Injection from Excited Semiconductor into Metal Oxides

The primary photochemical event leading to photocurrent generation in QDSCs is the charge separation at the metal

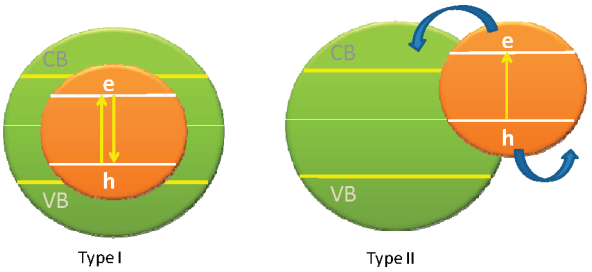

FIGURE 3. Manipulation of band alignment to direct the charge separation in semiconductor heterostructures.

chalcogenide–metal oxide interface. Since the early demonstration of the improved charge separation in CdS–ZnO and CdS–TiO_2 coupled semiconductors,[26,27] efforts have been made to design type I and type II semiconductor assemblies (Figure 3).

The matching of the band energies of the two semiconductors facilitates desired functionality either to induce electron–hole recombination (e.g., light-emitting diodes) or to improve charge separation by driving electrons and holes in two different nanoparticles (e.g., quantum dot solar cells). In each instance where semiconductor nanocrystals are implemented into a practical device, photoinduced electron transfer reactions are intimately involved, and they dictate overall functionality.

CdSe and CdS nanocrystals are convenient to study the energy gap dependence of photoinduced electron transfer between two semiconductor nanocrystals.[29,30] Using a series of CdSe quantum dot donors (sizes 2.8, 3.3, 4.0, and 4.2 nm) examination of electron transfer from CdSe quantum dots to metal oxides (SnO_2, TiO_2, and ZnO) has been conducted.[28] Apparent electron transfer rate constants showed strong dependence on change in system free energy, exhibiting a sharp rise at small driving forces followed by a modest rise further away from the characteristic reorganization energy (Figure 4). The observed trend agrees with the predicted behavior of electron transfer from a single quantum state to a continuum of electron-accepting states, such as those present in the conduction band of a metal oxide nanoparticle. The electron transfer rates for electron injection from four different sizes of CdSe quantum dots to three unique metal oxide species ranged from 1.9×10^{10} to 4.6×10^{11} s^{-1}, and trends generally agreed with Marcus theory of heterogeneous electron transfer process.[31,32] In contrast with dye sensitized metal oxide films, no room temperature hot electron injection was observed in these experiments.

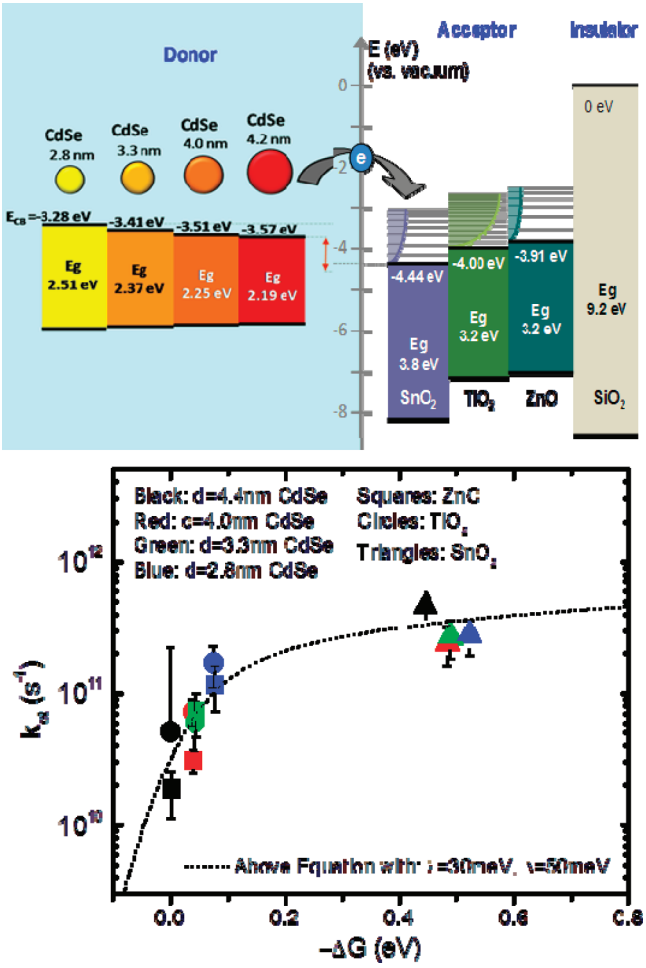

FIGURE 4. (top) Band energy diagram of different size CdSe nanoparticles and metal oxides. (bottom) Global plot of electron transfer rate constant versus free energy for all CdSe (donor) to metal oxide (acceptor). The trace is a theoretical fit based on Marcus many-state model with reorganization energy, $\lambda = 10$ meV, and defect distribution, $\Delta = 50$ meV. Reproduced with permission from ref 28. Copyright 2011 National Academy Press.

Effect of Linker Molecules on the Electron Injection Process

Another aspect to consider is the molecular linkage between the particles, which can slow the electron transfer based on the alkyl chain length.[33,34] Deposition of colloidal semiconductors from solution is a simple approach for achieving uniformly sized QDs on a TiO_2 surface. It is achieved through direct adsorption of QDs on TiO_2 or with the assistance of a molecular linker such as 3-mercaptopropionic acid (MPA), Figure 5.[35,36] Removal of surface-bound trioctylphosphine oxide, as well as use of MPA as a molecular linker, improves the adsorption of toluene-suspended QDs on TiO_2 films. The adsorption constants, K_{ad}, for submonolayer coverage were $(6.7 \pm 2.7) \times 10^3$ M^{-1} for direct adsorption and $(5.9 \pm 2.0) \times 10^4$ M^{-1} for MPA-linked assemblies.[36]

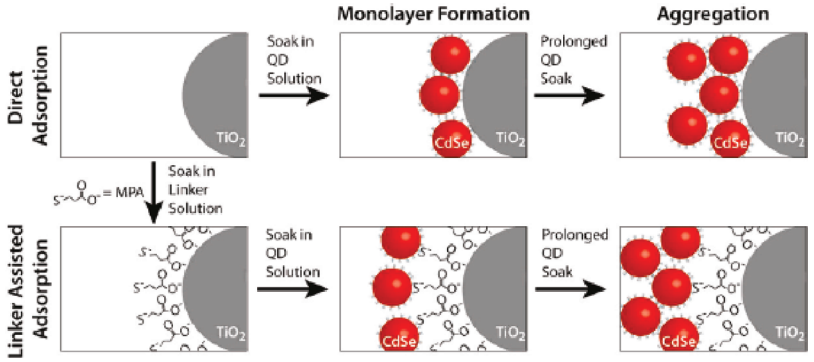

FIGURE 5. Linker-assisted and direct adsorption of QD on TiO_2. Submonolayer formation is followed by particle aggregation onto already-adsorbed quantum dots. Reproduced from ref 36. Copyright 2011 American Chemical Society.

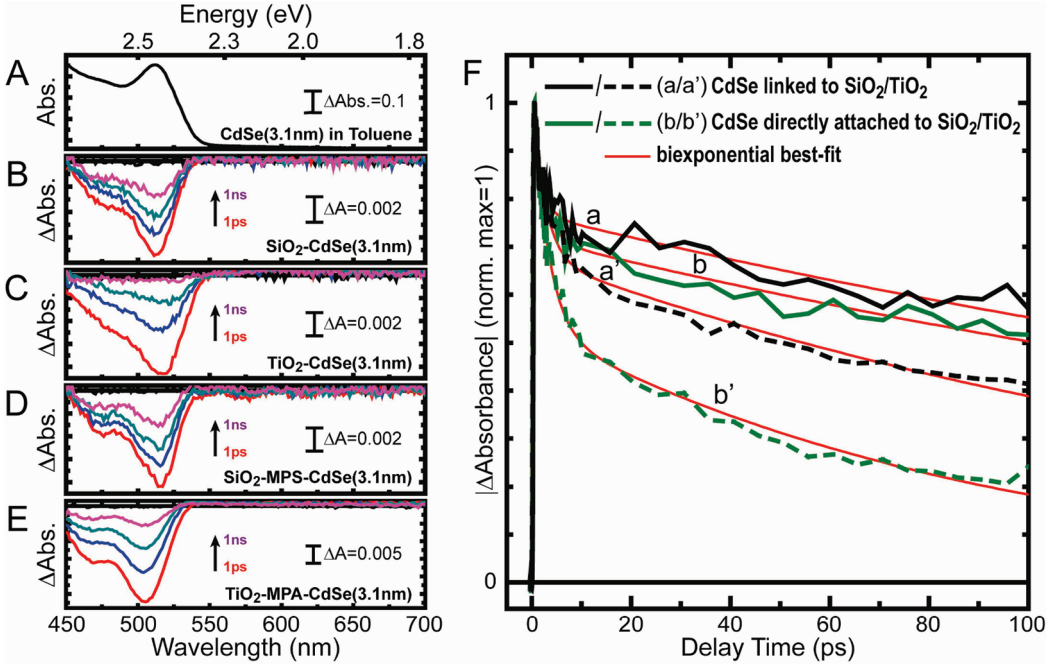

FIGURE 6. (A) Absorbance spectrum of ($d = 3.1$ nm) CdSe quantum dots in toluene solution. (B–E) Transient absorption spectra recorded following 387 nm laser pulse excitation of CdSe QDs attached to SiO_2/TiO_2 in a linkerless (B, C) and linked (D, E) fashion. The pump–probe delay times were 1, 10, 100, and 1000 ps (magenta). (F) Kinetic traces of B–E at the characteristic first excitonic peak of CdSe demonstrate the quenching of the excited state in the presence of TiO_2 acceptor. Reproduced from ref 36. Copyright 2011 American Chemical Society.

By attaching the same batch of QDs to TiO_2, a material that readily accepts electrons from the CdSe conduction band, we were able to probe the relaxation kinetics with the additional pathway of electron transfer.[36] The kinetic traces of each film are shown in Figure 6F. The apparent electron transfer rate constants determined from the transient bleaching recovery of CdSe QDs attached to TiO_2 nanoparticles in a linked and linkerless fashion were 2.3×10^9 and 7.2×10^9 s^{-1}, respectively. Given that the mechanism for electron transfer in the case of CdSe QDs on TiO_2 nanoparticles involves tunneling through the QD–metal oxide junction, we expect the transfer rate in the case of directly adsorbed QDs to be greater than that of those attached with a linker molecule. Previously, Watson and co-workers reported an increase in electron transfer rate from CdS QDs to TiO_2 nanoparticles with shorter mercaptoalkanoic acid chain length[37] It should be noted these studies were carried out with nanosecond time resolution and it did not compare the results with CdSe QDs directly attached to TiO_2. The picosecond time resolution presented in Figure 6 shows the electron transfer on the ultrafast time scale, the region that showcases the majority of temporal transient dynamics. In addition to electron transfer, the aggregation effects can also

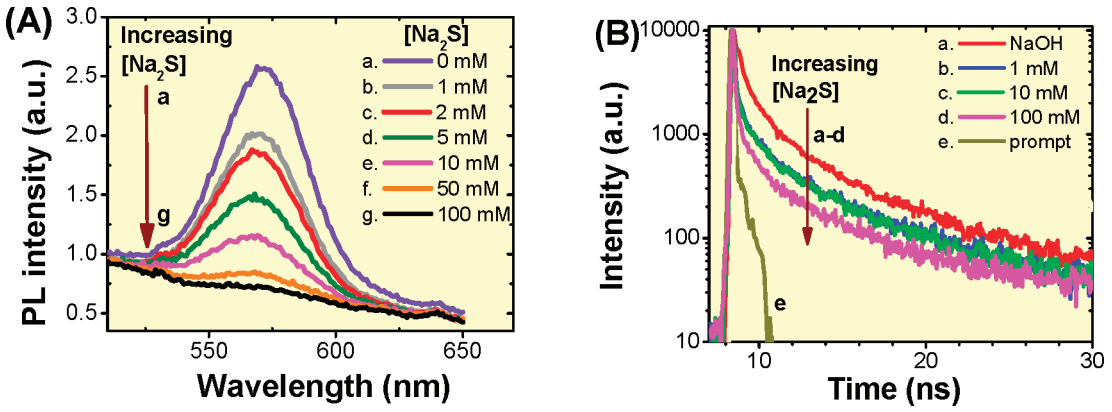

FIGURE 7. (A) Steady-state photoluminescence spectra of CdSe–SiO_2 film in contact with aqueous NaOH (pH = 13) solution containing (a) 0, (b) 1, (c) 2, (d) 5, (e) 10, (f) 50, and (g) 100 mM of Na_2S. The emission spectra were recorded using 390 nm excitation. (B) Emission decay monitored at 580 nm of CdSe quantum dots anchored on SiO_2 film in contact with NaOH solution (pH = 13) containing (a) 0, (b) 1, (c) 10, and (d) 100 mM Na_2S. Profile e corresponds to "prompt" instrument response measured against a blank SiO_2 film. The excitation wavelength was 373 nm. Reproduced from ref 42. Copyright 2011 American Chemical Society.

contribute to deactivation via energy transfer between two adjacent CdSe particles.

It is interesting to note that despite the presumably intimate contact for directly adsorbed QDs, k_{ET} increased by only a factor of 3. In terms of the probability of electron tunneling, which decreases exponentially with increasing distance, one would expect a greater enhancement of k_{ET} with direct attachment. We speculate that while the enhancement observed here is due to an increasingly intimate contact between the QD and TiO_2 species, even linkerless attachment results in contact that may be hindered by an energetic barrier.

The Hole Transfer at Irradiated Semiconductor Nanoparticles

The redox couple plays an important role in the regeneration of the semiconductor by scavenging photogenerated holes.[3] To date, the sulfide/polysulfide redox couple has remained a preferred choice because it assists in delivering high open circuit voltage and stability of solar cell operation.[38–40] Surface interaction between the organic molecules and the semiconductor also dictates the excited state dynamics.[41] For example, ligand exchange of surface-bound dodecylamine with mercaptopropionic acid has been shown to quench the bandgap emission and create Se vacancies.[41]

The emission of CdSe deposited on an inert oxide such as SiO_2 is useful to monitor the hole transfer at the CdSe interface.[42,43] In the absence of Na_2S, the CdSe exhibits a natural decay as it undergoes electron–hole recombination. In the presence of Na_2S, hole transfer to S^{2-} competes with the electron–hole recombination processes. The apparent rate constant obtained from the emission decay corresponds to $8.5 \times 10^7\ s^{-1}$ for the hole transfer to S^{2-} (Figure 7).[42] This value is 2–3 orders of magnitude lower than the electron injection from excited CdSe into TiO_2 and other oxide semiconductors.[28,30] Disparity between the electron and hole scavenging rate further leads to accumulation of holes within the CdSe QD, thus increasing the rate of electron–hole recombination.

Charge Recombination at the Semiconductor–Electrolyte Interface

It has been shown previously that the hole trapping and hole scavenging by S^{2-} produce $S^{\bullet-}$ radicals following the excitation of CdS or reaction with oxidizing radicals such as hydroxyl radicals.[44,45] Figure 8A shows the transient absorption spectra recorded following 532 nm laser pulse excitation of TiO_2–CdSe films immersed in 0.1 M Na_2S solution. The formation of $S^{\bullet-}$ is marked by a broad absorption in the visible 450–650 nm region.[46] As the photogenerated electrons are transferred to TiO_2 following charge separation, the holes accumulated within the CdSe are scavenged by the S^{2-} ions in the electrolyte to produce $S^{\bullet-}$ radical. The sulfide radical quickly complexes with S^{2-} ions and generates polysulfide radical (denoted as $(S_{n+1})^{\bullet-}$ in reaction 1).

$$S^{\bullet-} + nS^{2-} \rightarrow \rightarrow (S_{n+1})^{\bullet-} \qquad (1)$$

Figure 8B shows transient absorption decays at 590 and 550 nm, which represent the decay of $S^{\bullet-}$ radical and bleaching recovery of CdSe, respectively. The $S^{\bullet-}$ radicals

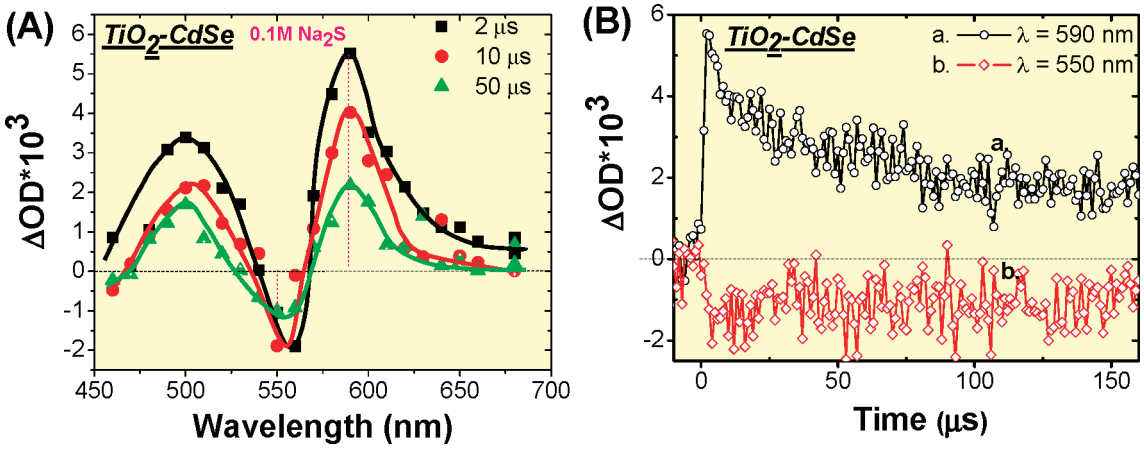

FIGURE 8. (A) Transient absorption spectra following 532 nm laser pulse excitation of CdSe–TiO_2 film in 0.1 M Na_2S solution. (B) Kinetic profiles of CdSe–TiO_2 film in contact with 0.1 M Na_2S at probe wavelengths of 550 and 590 nm. Reproduced from ref 42. Copyright 2011 American Chemical Society.

decay via recombination reaction with electrons that were injected into TiO_2 (reaction 2).

$$(S_{n+1})^{\bullet -} + TiO_2(e) \rightarrow (S_{n+1})^{2-} \quad (2)$$

From the transient decay at 590 nm, we obtain an average lifetime of 193 μs for $S^{\bullet -}$ radicals generated at the CdSe surface, which corresponds to a rate constant of 5.2×10^3 s^{-1} for the back electron transfer between electrons in the TiO_2 and $S^{\bullet -}$ radicals. This rate constant is at least 2 orders of magnitude greater than the one observed for TiO_2(e) and I_3^- in the regeneration step of dye sensitized solar cells. The faster recombination rate constant observed for reaction 2 is one of the major hurdles that needs to be taken into account when designing quantum dot solar cells. Addition of an oxidized counterpart (e.g., S or Se) to the electrolyte, though beneficial for improving the electron discharge at the counter electrode, adversely affects the cell performance because of increased electron recombination at the CdSe–TiO_2 electrode interface.

Anodic Corrosion

The consequence of a slow rate of hole scavenging by the redox couple is reflected in anodic corrosion. This is especially significant for CdTe system, which undergoes anodic corrosion within minutes of visible light irradiation in sulfide/polysulfide medium.[50] CdSe on the other hand undergoes small changes in the sulfide medium to form a thin layer of cadmium sulfoselenide.[42] The formation of this layer has been confirmed from the red shift in the absorption as well as elemental analysis of the irradiated electrodes. The formation of the cadmium sulfoselenide layer acts as a barrier to prevent further corrosion as well as suppress back electron transfer to the oxidized form of the redox couple. As a result of this barrier layer, one observes significant improvement in the CdSe sensitized solar cells with sulfide/polysulfide electrolyte and delivery of stable photocurrent over a long period time. Coating the CdSe with a ZnS barrier layer is another approach other researchers have found to be useful in maintaining the photostability of the solar cell.[51]

Redox Processes at Counter Electrode

In order to maximize the performance of QDSCs, one needs to discharge the electrons quickly at the counter electrode. While polysulfide electrolyte is beneficial to the stability of the photoanode in liquid junction QDSCs, power conversion efficiencies have remained low. A general polysulfide reduction is represented in reaction 3.

$$S_n^{2-} + e^- \rightarrow nS^{2-} \quad (3)$$

Sulfur compounds are known to chemisorb on platinum surfaces and induce poisoning effects toward electrode performance.[52] A poor charge transfer rate at the counter electrode results in high overpotential for the reduction reaction, which creates a bottleneck for the electron flow, thereby promoting back electron transfer at the photoanode. These effects are realized from the low current density and fill factor of the QDSC.[42] Figure 9 depicts a schematic illustration of fast and slow response of RGO–Cu_2S and platinum electrodes toward polysulfide reduction during the operation of QDSCs.

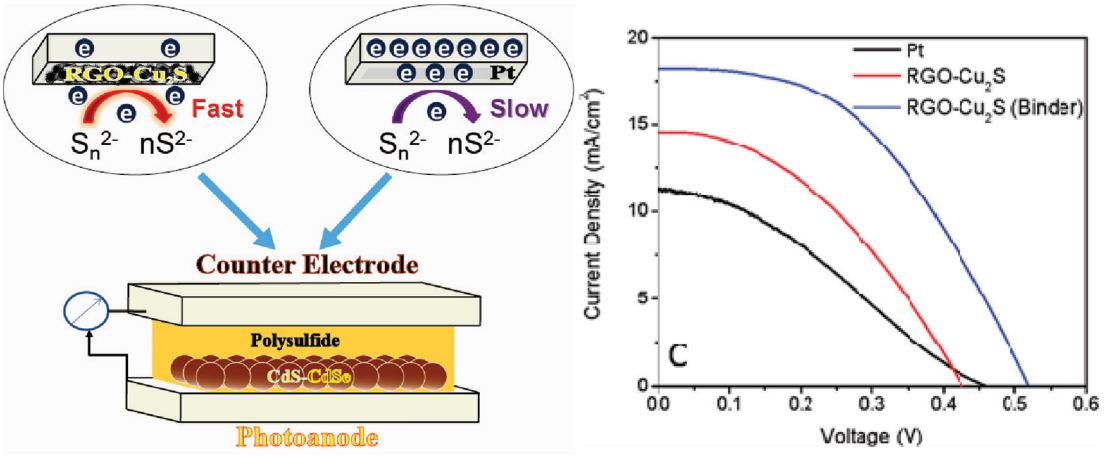

FIGURE 9. (left) A QDSC depicting the comparison of the kinetics of the polysulfide couple at Pt and RGO–Cu_2S counter electrodes. (right) The *I*–*V* characteristics of QDSCs employing Pt and RGO–Cu_2S counter electrodes Reproduced from ref 54. Copyright 2011 American Chemical Society.

Prior research shows that metal chalcogenides such as CoS, PbS, and Cu_2S exhibit high electrocatalytic activity for polysulfide reduction with Cu_2S.[53] Although metal foils of Cu, Co, or Pb can be exposed to sulfide solution and obtain a layer of metal sulfide, this preparative method suffers from continual corrosion resulting in mechanical instability. We recently succeeded in developing a composite material consisting of reduced graphene oxide (RGO) and Cu_2S.[54] The high surface area of the 2-D structure promotes high numbers of the Cu_2S reactive sites spread across the surface of RGO sheets. RGO serves to shuttle electrons across the 2-D mat to the sulfide-active Cu_2S catalyst sites where the electrons are used to reduce the oxidized polysulfide.

The effectiveness of the RGO–Cu_2S-binder as the superior counter electrode is reflected in higher power conversion efficiency for QDSC under AM1.5 illumination (see, for example, *I*–*V* characteristics in Figure 9). An efficiency value of 4.4% with RGO–Cu_2S counter electrode compared with 1.6% with Pt counter electrodes was achieved. The relatively high external quantum efficiency (~90% at 400 nm) obtained with RGO–Cu_2S counter electrode shows nearly ideal operation of QDSC for conversion of incident photons to current at low incident light intensities.

Toward the Goal of Achieving 10% Efficient QDSCs

Quantum dot solar cells offer opportunities to manage photon harvesting through tuning of photoresponse as well as utilization of multiple electron generation achieved through high-energy photon excitation.[13,55] QDSCs, which typically exhibit power conversion efficiency around 5%,[51,56–58] have yet to deliver efficiencies that are comparable to 12% of their counterpart, dye sensitized solar cells.[59–61] It is imperative that the efficiency of QDSCs be ~10% in order to make them market competitive. The factors that limit overall power conversion efficiency of QDSCs include limited absorption of the incident light, slow hole transfer rate, back electron transfer to the oxidized form of the redox couple, and low fill factors arising from poor counter electrode performance. To date, the sulfide/polysulfide redox couple has been the choice for most liquid junction QDSCs because it provides desirable stability during irradiation. Slow hole regeneration and anodic corrosion of the QDs limits the use of other common redox couples such as I^-/I_3^-.[49,62]

Many recent reports claim high efficiency for QDSCs by spiking 70% methanol in the electrolyte.[63] It should be noted that methanol is a sacrificial electron donor. In addition, oxidized methoxy radicals also serve as electron donors. The current doubling effect of methanol in photoelectrochemical cells is well documented.[64] Hence, it is important to weigh such high efficiency claims while comparing the performance with regenerative QDSCs.

Supersensitization of QDs such as CdS with an organic dye absorbing in the infrared region provides a good strategy to extend the absorption as well as to manipulate charge recombination at the electrolyte interface. Recently, Zaban et al.[65,66] reported the CdS quantum dot–TiO_2–dye bilayer cosensitization that facilitated the use of I^-/I_3^- couple. Similarly, a squaraine dye was employed to selectively capture photons in the NIR region and CdS QD in the visible region.[67] Opportunities also exist to utilize semiconductor nanowire–QD composites or coaxial nanowires in solar cells.

CdSe–C_{60} composites have also been shown to induce charge separation under bandgap irradiation.[23,68] Other

carbon nanostructures such as carbon nanotubes or reduced graphene oxide can serve as conducting scaffolds and facilitate electron transport within the mesoscopic semiconductor film thus decreasing the probability of recombination losses at the grain boundaries. The ability of these carbon nanostructures to capture and transport electrons has been monitored using charge equilibration studies.[69−71] Their role in modifying the properties of QDSCs needs to be explored with greater detail. A major limitation is the light filtering effect of carbon nanostructures, which in turn allows their incorporation in semiconductor films only in small quantities.

Another approach for modifying the intrinsic properties of semiconductor nanocrystals is to introduce dopants.[72,73] By doping optically active transition metal ions, for example, Mn^{2+}, it is possible to modify the electronic and photophysical properties of QDs.[74−76] The dopant creates electronic states in the midgap region of the QD thus altering the charge separation and recombination dynamics. In addition, it is also possible to tune the optical and electronic properties of semiconductor nanocrystals by controlling the type and concentration of dopants. Synthesis of Mn-doped II−VI semiconductor QDs and their photophysical properties have been the subject of recent reports.[77−79] The Mn d−d transition ($^4T_1-{}^6A_1$) in these doped systems is both spin and orbitally forbidden and thus results in a long lifetime of several hundreds of microseconds.[80,81] By careful manipulation of doped semiconductor architecture, it should be possible to utilize long-lived charge carriers for boosting the efficiency of QDSCs. A recent report of achieving 5.4% efficiency for a Mn-doped solar cell demonstrates the effectiveness of doped semiconductor nanocrystals.[82]

A recent effort to develop "Sun-Believable" paint using CdS−CdSe−TiO_2 composite nanoparticles is another major step toward the development of a transformative technology of QDSCs.[83] During the last 3−4 years ,we have seen an increase in the photoconversion efficiency from less than 1% to over 5%. Mechanistic and kinetic understanding of charge transfer processes have identified areas to address limiting factors in QDSCs. It is important that interfacial charge transfer processes be taken into account while designing economically viable solar cells.

I would like to acknowledge the past and present co-workers whose work in part is discussed in this Account. The research described herein was supported by the Division of Chemical Sciences, Geosciences, and Biosciences, Office of Basic Energy Sciences, of the U.S. Department of Energy through Award DE-FC02-04ER15533. This is contribution number NDRL 4910 from the Notre Dame Radiation Laboratory.

BIOGRAPHICAL INFORMATION

Prashant V. Kamat is a Rev. John A. Zahm Professor of Science in the Department of Chemistry and Biochemistry and the Radiation Laboratory and a Concurrent Professor in the Department of Chemical and Biomolecular Engineering, University of Notre Dame. His major research interests are in the areas of photoinduced charge-transfer processes in semiconductor nanocrystal-based architectures, photocatalytic aspects of metal nanoparticles and carbon nanostructures, and designing light-harvesting assemblies for next generation solar cells. See http://www.nd.edu/~kamatlab for recent research activities.

FOOTNOTES

*E-mail: pkamat@nd.edu.
The authors declare no competing financial interest.

REFERENCES

1 Kamat, P. V. Meeting the Clean Energy Demand: Nanostructure Architectures for Solar Energy Conversion. *J. Phys. Chem. C* **2007**, *111*, 2834–2860.
2 Kamat, P. V. Quantum Dot Solar Cells. Semiconductor Nanocrystals as Light Harvesters. *J. Phys. Chem. C* **2008**, *112*, 18737–18753.
3 Kamat, P. V.; Tvrdy, K.; Baker, D. R.; Radich, J. G. Beyond Photovoltaics: Semiconductor Nanoarchitectures for Liquid Junction Solar Cells. *Chem. Rev.* **2010**, *110*, 6664–6688.
4 Mora-Sero, I.; Bisquert, J. Breakthroughs in the Development of Semiconductor Sensitized Solar Cells. *J. Phys. Chem. Lett.* **2010**, *1*, 3046–3052.
5 Buhbut, S.; Itzhakov, S.; Oron, D.; Zaban, A. Quantum Dot Antennas for Photoelectrochemical Solar Cells. *J. Phys. Chem. Lett.* **2011**, *2*, 1917–1924.
6 Kramer, I. J.; Sargent, E. H. Colloidal Quantum Dot Photovoltaics: A Path Forward. *ACS Nano* **2011**, *5*, 8506–8514.
7 Nozik, A. J.; Beard, M. C.; Luther, J. M.; Law, M.; Ellingson, R. J.; Johnson, J. C. Semiconductor Quantum Dots and Quantum Dot Arrays and Applications of Multiple Exciton Generation to Third-Generation Photovoltaic Solar Cells. *Chem. Rev.* **2010**, *110*, 6873–6890.
8 Smotkin, E. S.; Cervera-March, S.; Bard, A. J.; Campion, A.; Fox, M. A.; Mallouk, T.; Webber, S. E.; White, J. M. Bipolar Cadmium Selenide/Cobalt(II) Sulfide Semiconductor Photoelectrode Arrays for Unassisted Photolytic Water Splitting. *J. Phys. Chem.* **1987**, *91*, 6–8.
9 Frame, F. A.; Osterloh, F. E. CdSe-MoS_2: A Quantum Size-Confined Photocatalyst for Hydrogen Evolution from Water under Visible Light. *J. Phys. Chem. C* **2010**, *114*, 10628–10633.
10 Liu, L.; Hensel, J.; Fitzmorris, R. C.; Li, Y.; Zhang, J. Z. Preparation and Photoelectrochemical Properties of CdSe/TiO2 Hybrid Mesoporous Structures. *J. Phys. Chem. Lett.* **2010**, *1*, 155–160.
11 Amirav, L.; Alivisatos, A. P. Photocatalytic Hydrogen Production with Tunable Nanorod Heterostructures. *J. Phys. Chem. Lett.* **2010**, *1*, 1051–1054.
12 Wang, C.; Thompson, R. L.; Baltrus, J.; Matranga, C. Visible Light Photoreduction of CO_2 Using CdSe/Pt/TiO_2 Heterostructured Catalysts. *J. Phys. Chem. Lett.* **2010**, *1*, 48–53.
13 Beard, M. C. Multiple Exciton Generation in Semiconductor Quantum Dots. *J. Phys. Chem. Lett.* **2011**, *2*, 1282–1288.
14 Hetsch, F.; Xu, X.; Wang, H.; Kershaw, S. V.; Rogach, A. L. Semiconductor Nanocrystal Quantum Dots as Solar Cell Components and Photosensitizers: Material, Charge Transfer, and Separation Aspects of Some Device Topologies. *J. Phys. Chem. Lett.* **2011**, *2*, 1879–1887.
15 Yu, Y.; Kamat, P. V.; Kuno, M. A CdSe Nanowire/Quantum Dot Hybrid Architecture for Improving Solar Cell Performance. *Adv. Funct. Mater.* **2010**, *20*, 1464–1472.
16 Giblin, J.; Kuno, M. Nanostructure Absorption: A Comparative Study of Nanowire and Colloidal Quantum Dot Absorption Cross Sections. *J. Phys. Chem. Lett.* **2010**, *1*, 3340–3348.
17 Baker, D. R.; Kamat, P. V. Photosensitization of TiO_2 Nanostructures with CdS Quantum Dots. Particulate versus Tubular Support Architectures. *Adv. Funct. Mater.* **2009**, *19*, 805–811.
18 Vogel, R.; Pohl, K.; Weller, H. Sensitization of Highly Porous, Polycrystalline TiO_2 Electrodes by Quantum Sized CdS. *Chem. Phys. Lett.* **1990**, *174*, 241–246.

19 Mora-Seró, I.; Giménez, S.; Moehl, T.; Fabregat-Santiago, F.; Lana-Villareal, T.; Gómez, R.; Bisquert, J. Factors Determining the Photovoltaic Performance of a CdSe Quantum Dot Sensitized Solar Cell: The role of the Linker Molecule and of the Counter Electrode. *Nanotechnol. Mesostruct. Mater.* **2008**, *19*, No. 424007.

20 Guijarro, N.; Lana-Villarreal, T.; Mora-Sero, I.; Bisquert, J.; Gomez, R. CdSe Quantum Dot-Sensitized TiO_2 Electrodes: Effect of Quantum Dot Coverage and Mode of Attachment. *J. Phys. Chem. C* **2009**, *113*, 4208–4214.

21 Ham, D.; Mishra, K. K.; Rajeshwar, K. Anodic Electrosynthesis of Cadmium Selenide Thin Films. *J. Electrochem. Soc.* **1991**, *138*, 100–108.

22 Yochelis, S.; Hodes, G. Nanocrystalline CdSe Formation by Direct Reaction between Cd Ions and Selenosulfate Solution. *Chem. Mater.* **2004**, *16*, 2740–2744.

23 Brown, P.; Kamat, P. V. Quantum Dot Solar Cells. Electrophoretic Deposition of CdSe–C_{60} Composite Films and Capture of Photogenerated Electrons with nC_{60} Cluster Shell. *J. Am. Chem. Soc.* **2008**, *130*, 8890–8891.

24 Robel, I.; Subramanian, V.; Kuno, M.; Kamat, P. V. Quantum Dot Solar Cells. Harvesting Light Energy with CdSe Nanocrystals Molecularly Linked to Mesoscopic TiO_2 Films. *J. Am. Chem. Soc.* **2006**, *128*, 2385–2393.

25 Watson, D. F. Linker-Assisted Assembly and Interfacial Electron-Transfer Reactivity of Quantum Dota Substrate Architectures. *J. Phys. Chem. Lett.* **2010**, *1*, 2299–2309.

26 Spanhel, L.; Weller, H.; Henglein, A. Photochemistry of Semiconductor Colloids. 22. Electron Injection from Illuminated CdS into Attached TiO_2 and ZnO Particles. *J. Am. Chem. Soc.* **1987**, *109*, 6632–6635.

27 Gopidas, K. R.; Bohorquez, M.; Kamat, P. V. Photoelectrochemistry in Semiconductor Particulate Systems. 16. Photophysical and Photochemical Aspects of Coupled Semiconductors. Charge-transfer Processes in Colloidal CdS–TiO_2 and CdS–AgI Systems. *J. Phys. Chem.* **1990**, *94*, 6435–6440.

28 Tvrdy, K.; Frantszov, P.; Kamat, P. V. Photoinduced Electron Transfer from Semiconductor Quantum Dots to Metal Oxide Nanoparticles. *Proc. Natl. Acad. Sci. U.S.A.* **2011**, *108*, 29–34.

29 Sant, P. A.; Kamat, P. V. Inter-Particle Electron Transfer between Size-Quantized CdS and TiO_2 Semiconductor Nanoclusters. *Phys. Chem. Chem. Phys.* **2002**, *4*, 198–203.

30 Robel, I.; Kuno, M.; Kamat, P. V. Size-Dependent Electron Injection from Excited CdSe Quantum Dots into TiO_2 Nanoparticles. *J. Am. Chem. Soc.* **2007**, *129*, 4136–4137.

31 Marcus, R. A. Theory of Oxidation-Reduction Reactions Involving Electron Transfer. 5. Comparison and Properties of Electrochemical and Chemical Rate Constants. *J. Phys. Chem.* **1963**, *67*, 853–857.

32 Marcus, R. A. A Theory of Electron Transfer Processes at Electrodes. *J. Electrochem. Soc.* **1959**, *106*, C71–C72.

33 Kongkanand, A.; Tvrdy, K.; Takechi, K.; Kuno, M. K.; Kamat, P. V. Quantum Dot Solar Cells. Tuning Photoresponse through Size and Shape Control of CdSe–TiO_2 Architecture. *J. Am. Chem. Soc.* **2008**, *130*, 4007–4015.

34 Hyun, B.-R.; Bartnik, A. C.; Sun, L.; Hanrath, T.; Wise, F. W. Control of Electron Transfer from Lead-Salt Nanocrystals to TiO_2. *Nano Lett.* **2011**, *11*, 2126–2132.

35 Mann, J. R.; Watson, D. F. Adsorption of CdSe Nanoparticles to Thiolated TiO_2 Surfaces: Influence of Intralayer Disulfide Formation on CdSe Surface Coverage. *Langmuir* **2007**, *23*, 10924–10928.

36 Pernik, D.; Tvrdy, K.; Radich, J. G.; Kamat, P. V. Tracking the Adsorption and Electron Injection Rates of CdSe Quantum Dots on TiO_2: Linked Versus Direct Attachment. *J. Phys. Chem. C* **2011**, *115*, 13511–13519.

37 Dibbell, R. S.; Watson, D. F. Distance-Dependent Electron Transfer in Tethered Assemblies of CdS Quantum Dots and TiO_2 Nanoparticles. *J. Phys. Chem. C* **2009**, *113*, 3139–3149.

38 Ellis, A. B.; Kaiser, S. W.; Wrighton, M. S. Visible Light to Electrical Energy Conversion. Stable Cadmium Sulfide and Cadmium Selenide Photoelectrodes in Aqueous Electrolytes. *J. Am. Chem. Soc.* **1976**, *98*, 1635–1637.

39 Tenne, R.; Lando, D.; Mirovsky, Y.; Mueller, N.; Manassen, J.; Cahen, D.; Hodes, G. The Relation between Performance and Stability of Cd-Chalcogenide/Polysulfide Photoelectrochemical Cells. The Effect of Potential. *J. Electroanal. Chem., Interfacial Electrochem.* **1983**, *143*, 103–112.

40 Vainas, B.; Hodes, G.; Dubow, J. A Photocathodic Effect at the CdS-Electrolyte Interface. *J. Electroanal. Chem., Interfacial Electrochem.* **1981**, *130*, 391–394.

41 Baker, D. R.; Kamat, P. V. Tuning the Emission of CdSe Quantum Dots by Controlled Trap Enhancement. *Langmuir* **2010**, *26*, 11272–11276.

42 Chakrapani, V.; Baker, D.; Kamat, P. V. Understanding the Role of the Sulfide Redox Couple (S^{2-}/S_n^{2-}) in Quantum Dot Sensitized Solar Cells. *J. Am. Chem. Soc.* **2011**, *133*, 9607–9615.

43 Chakrapani, V.; Tvrdy, K.; Kamat, P. V. Modulation of Electron Injection in CdSe–TiO_2 System through Medium Alkalinity. *J. Am. Chem. Soc.* **2010**, *132*, 1228–1229.

44 Kamat, P. V.; Ebbesen, T. W.; Dimitrijevic, N. M.; Nozik, A. J. Photoelectrochemistry in Semiconductor Particulate Systems. Part 12. Primary Photochemical Events in CdS Semiconductor Colloids as Probed by Picosecond Laser Flash Photolysis, Transient Bleaching. *Chem. Phys. Lett.* **1989**, *157*, 384–389.

45 Kamat, P. V.; Gopidas, K. R.; Dimitrijevic, N. M. Picosecond Charge Transfer Processes in Ultrasmall CdS and CdSe Semiconductor Particles. *Mol. Cryst. Liq. Cryst.* **1990**, *183*, 439–445.

46 Stroyuk, A. L.; Raevskaya, A. E.; Kuchmii, S. Y. Oxidation of Polysulfide Ions Induced by CdS Nanoparticles under Pulsed Photolysis Conditions. *Theor. Exp. Chem.* **2004**, *40*, 130–135.

47 Green, A. N. M.; Chandler, R. E.; Haque, S. A.; Nelson, J.; Durrant, J. R. Transient Absorption Studies and Numerical Modeling of Iodine Photoreduction by Nanocrystalline TiO_2 Films. *J. Phys. Chem. B* **2005**, *109*, 142–150.

48 Peter, L. M. Characterization and Modeling of Dye-Sensitized Solar Cells. *J. Phys. Chem. C* **2007**, *111*, 6601–6612.

49 Rowley, J. G.; Farnum, B. H.; Ardo, S.; Meyer, G. J. Making and Breaking I–I Bonds for Solar Energy Conversion. *J. Phys. Chem. Lett.* **2010**, *1*, 3132–3140.

50 Bang, J. H.; Kamat, P. V. Quantum Dot Sensitized Solar Cells. A Tale of Two Semiconductor Nanocrystals: CdSe and CdTe. *ACS Nano* **2009**, *3*, 1467–1476.

51 Shen, Q.; Kobayashi, J.; Diguna, L. J.; Toyoda, T. Effect of ZnS Coating on the Photovoltaic Properties of CdSe Quantum Dot-Sensitized Solar Cells. *J. Appl. Phys.* **2008**, *103*, No. 084304.

52 Loucka, T. Adsorption and Oxidation of Organic Compounds on a Platinum-Electrode Partly Covered by Adsorbed Sulfur. *J. Electroanal. Chem.* **1972**, *36*, 355–367.

53 Hodes, G.; Manassen, J.; Cahen, D. Electrocatalytic Electrodes for the Polysulfide Redox System. *J. Electrochem. Soc.* **1980**, *127*, 544–549.

54 Radich, J. G.; Dwyer, R.; Kamat, P. V. Cu_2S Reduced Graphene Oxide Composite for High-Efficiency Quantum Dot Solar Cells. Overcoming the Redox Limitations of S_2^-/S_n^{2-} at the Counter Electrode. *J. Phys. Chem. Lett.* **2011**, *2*, 2453–2460.

55 Semonin, O. E.; Luther, J. M.; Choi, S.; Chen, H. Y.; Gao, J. B.; Nozik, A. J.; Beard, M. C. Peak External Photocurrent Quantum Efficiency Exceeding 100% via MEG in a Quantum Dot Solar Cell. *Science* **2011**, *334*, 1530–1533.

56 Diguna, L. J.; Shen, Q.; Kobayashi, J.; Toyoda, T. High Efficiency of CdSe Quantum-Dot-Sensitized TiO_2 Inverse Opal Solar Cells. *Appl. Phys. Lett.* **2007**, *91*, No. 023116.

57 Barea, E. M.; Shalom, M.; Giménez, S.; Hod, I.; Mora-Seró, I. n.; Zaban, A.; Bisquert, J. Design of Injection and Recombination in Quantum Dot Sensitized Solar Cells. *J. Am. Chem. Soc.* **2010**, *132*, 6834–6839.

58 Gonzalez-Pedro, V.; Xu, X.; Mora-Sero, I.; Bisquert, J. Modeling High-Efficiency Quantum Dot Sensitized Solar Cells. *ACS Nano* **2010**, *4*, 5783–5790.

59 Alstrum-Acevedo, J. H.; Brennaman, M. K.; Meyer, T. J. Chemical Approaches to Artificial Photosynthesis. *Inorg. Chem.* **2005**, *44*, 6802–6827.

60 Graetzel, M. Recent Advances in Sensitized Mesoscopic Solar Cells. *Acc. Chem. Res.* **2009**, *42*, 1788–1798.

61 Miyasaka, T. Toward Printable Sensitized Mesoscopic Solar Cells: Light-Harvesting Management with Thin TiO_2 Films. *J. Phys. Chem. Lett.* **2011**, *2*, 262–269.

62 Call, F.; Stolwijk, N. A. Impact of I_2 Additions on Iodide Transport in Polymer Electrolytes for Dye-Sensitized Solar Cells: Reduced Pair Formation versus a Grotthuss-Like Mechanism. *J. Phys. Chem. Lett.* **2010**, *1*, 2088–2093.

63 Yu, X.-Y.; Liao, J.-Y.; Qiu, K.-Q.; Kuang, D.-B.; Su, C.-Y. Dynamic Study of Highly Efficient CdS/CdSe Quantum Dot-Sensitized Solar Cells Fabricated by Electrodeposition. *ACS Nano* **2011**, *5*, 9494–9500.

64 Mandelbaum, P. A.; Regazzoni, A. E.; Blesa, M. A.; Bilmes, S. A. Photo-electro-oxidation of Alcohols on Titanium Dioxide Thin Film Electrodes. *J. Phys. Chem. B* **1999**, *103*, 5505–5511.

65 Shalom, M.; Albero, J.; Tachan, Z.; Martinez-Ferrero, E.; Zaban, A.; Palomares, E. Quantum Dot-Dye Bilayer-Sensitized Solar Cells: Breaking the Limits Imposed by the Low Absorbance of Dye Monolayers. *J. Phys. Chem. Lett.* **2010**, *1*, 1134–1138.

66 Buhbut, S.; Itzhakov, S.; Tauber, E.; Shalom, M.; Hod, I.; Geiger, T.; Garini, Y.; Oron, D.; Zaban, A. Built-in Quantum Dot Antennas in Dye-Sensitized Solar Cells. *ACS Nano* **2010**, *4*, 1293–1298.

67 Choi, H.; Nicolaescu, R.; Paek, S.; Ko, J.; Kamat, P. V. Supersensitization of CdS Quantum Dots with NIR Organic Dye: Towards the Design of Panchromatic Hybrid-Sensitized Solar Cells. *ACS Nano* **2011**, *5*, 9238–9245.

68 Bang, J. H.; Kamat, P. V. CdSe Quantum Dot-Fullerene Hybrid Nanocomposite for Solar Energy Conversion: Electron Transfer and Photoelectrochemistry. *ACS Nano* **2011**, *5*, 9421–9427.

69 Lightcap, I. V.; Kosel, T. H.; Kamat, P. V. Anchoring Semiconductor and Metal Nanoparticles on a 2-Dimensional Catalyst Mat. Storing and Shuttling Electrons with Reduced Graphene Oxide. *Nano Lett.* **2010**, *10*, 577–583.

70 Kamat, P. V. Graphene Based Nanoarchitectures. Anchoring Semiconductor and Metal Nanoparticles on a 2-Dimensional Carbon Support. *J. Phys. Chem. Lett.* **2010**, *1*, 520–527.

71 Farrow, B.; Kamat, P. V. CdSe Quantum Dot Sensitized Solar Cells. Shuttling Electrons through Stacked Carbon Nanocups. *J. Am. Chem. Soc.* **2009**, *131*, 11124–11131.

72 Pradhan, N.; Sarma, D. D. Advances in Light-Emitting Doped Semiconductor Nanocrystals. *J. Phys. Chem. Lett.* **2011**, *2*, 2818–2826.

73 Chikan, V. Challenges and Prospects of Electronic Doping of Colloidal Quantum Dots: Case Study of CdSe. *J. Phys. Chem. Lett.* **2011**, *2*, 2783–2789.

74 Jana, S.; Srivastava, B. B.; Pradhan, N. Correlation of Dopant States and Host Bandgap in Dual-Doped Semiconductor Nanocrystals. *J. Phys. Chem. Lett.* **2011**, *2*, 1747–1752.

75 Beaulac, R.; Archer, P. I.; Ochsenbein, S. T.; Gamelin, D. R. Mn(2+)-Doped CdSe Quantum Dots: New Inorganic Materials for Spin-Electronics and Spin-Photonics. *Adv. Funct. Mater.* **2008**, *18*, 3873–3891.

76 Zeng, R.; Rutherford, M.; Xie, R.; Zou, B.; Peng, X. Synthesis of Highly Emissive Mn-Doped ZnSe Nanocrystals without Pyrophoric Reagents. *Chem. Mater.* **2010**, *22*, 2107–2113.

77 Norris, D. J.; Efros, A. L.; Erwin, S. C. Doped Nanocrystals. *Science* **2008**, *319*, 1776–1779.

78 Karan, N. S.; Sarma, D. D.; Kadam, R. M.; Pradhan, N. Doping Transition Metal (Mn or Cu) Ions in Semiconductor Nanocrystals. *J. Phys. Chem. Lett.* **2010**, *1*, 2863–2866.

79 Nag, A.; Cherian, R.; Mahadevan, P.; Gopal, A. V.; Hazarika, A.; Mohan, A.; Vengurlekar, A. S.; Sarma, D. D. Size-Dependent Tuning of Mn(2+) d Emission in Mn(2+)-Doped CdS Nanocrystals: Bulk vs Surface. *J. Phys. Chem. C* **2010**, *114*, 18323–18329.

80 Beaulac, R.; Archer, P. I.; Liu, X. Y.; Lee, S.; Salley, G. M.; Dobrowolska, M.; Furdyna, J. K.; Gamelin, D. R. Spin-Polarizable Excitonic Luminescence in Colloidal Mn2+-Doped CdSe Quantum Dots. *Nano Lett.* **2008**, *8*, 1197–1201.

81 Vlaskin, V. A.; Janssen, N.; van Rijssel, J.; Beaulac, R.; Gamelin, D. R. Tunable Dual Emission in Doped Semiconductor Nanocrystals. *Nano Lett.* **2010**, *10*, 3670–3674.

82 Santra, P. K.; Kamat, P. V. Mn-Doped Quantum Dot Sensitized Solar Cells. A Strategy to Boost Efficiency over 5%. *J. Am. Chem. Soc.* **2012**, *134*, 2508–2511.

83 Genovese, M. P.; Lightcap, I. V.; Kamat, P. V. Sun-Believable Solar Paint. A Transformative One-Step Approach for Designing Nanocrystalline Solar Cells. *ACS Nano* **2012**, *6*, 865–872.